Journal of Catalysis 273 (2010) 191–198

Contents lists available at ScienceDirect

Journal of Catalysis

journal homepage: www.elsevier.com/locate/jcat

Catalytic performance of Au/ZnO nanocatalysts for CO oxidation

S.A.C. Carabineiro [a,*], B.F. Machado [a], R.R. Bacsa [b], P. Serp [b,**], G. Dražić [c], J.L. Faria [a], J.L. Figueiredo [a]

[a] Laboratory of Catalysis and Materials (LCM), Associate Laboratory LSRE/LCM, Chemical Engineering Department, Faculty of Engineering, University of Porto, Rua Dr. Roberto Frias s/n, 4200-465 Porto, Portugal
[b] Laboratoire de Chimie de Coordination du CNRS, ENSIACET, 4 Allée Monso-BP 44362, 31432 Toulouse, France
[c] Jozef Stefan Institute, Department of Nanostructured Materials, Jamova 39, SI-1000 Ljubljana, Slovenia

ARTICLE INFO

Article history:
Received 2 April 2010
Revised 20 May 2010
Accepted 21 May 2010
Available online 23 June 2010

Keywords:
Gold
Zinc oxide
Carbon monoxide
Oxidation
Chemical vapour deposition

ABSTRACT

Au was loaded (1% wt.) on three different ZnO supports, by three different methods: photodeposition, double impregnation and ultrasonication. Two commercial ZnO supports were used, along with a ZnO sample consisting of nanosized single crystals prepared by chemical vapour deposition. The samples were extensively characterised by various techniques. CO oxidation was used as a test reaction to compare the catalytic activity. The best results were obtained with ZnO prepared by chemical vapour deposition with Au loaded by ultrasonication that showed an activity of 2 $mol_{CO}\ g_{Au}^{-1}\ h^{-1}$ at room temperature. High-resolution electron microscopy images of the sample showed a number of gold nanocrystals epitaxially oriented on the ZnO rod. The unique catalyst–substrate interaction can be related to the increased catalytic activity of this sample, which was not observed for any of the others.

1. Introduction

When compared to other supports, ZnO has been less used as a carrier for gold catalysts [1,2]. Some examples of reactions catalysed by Au/ZnO materials include methanol synthesis [3], methanol steam-reforming to hydrogen [4], selective catalytic reduction of NO using propene [5], hydrogenation of CO_2 [6,7] or aldehydes [8,9], H_2O_2 synthesis [10], oxidation of salicylic alcohol [11], epoxidation of styrene to styrene oxide [12] and photocatalysis [13]. Few studies were carried out with Au/ZnO on CO oxidation [14–19] even though this is an intensively studied reaction with several other supports [1,2], and on related reactions, such as water gas shift [20] and preferential oxidation of CO in the presence of hydrogen (PROX) [21–27]. Moreover, Au/ZnO might be a promising system to use as a sensor for CO [28–30], VOCs [31], butane [32], hydrogen [33], oxygen [34] and for bio-active compounds [35].

Nevertheless, Wang et al. [16] found that Au/ZnO catalysts exhibit good catalytic activity and stability for CO oxidation at room temperature in the presence of water. When comparing Au/ZnO, Au/CuO and Au/CuO–ZnO catalysts prepared by a coprecipitation method, Hutchings et al. [15] found out that they were highly active for CO oxidation and capable of sustained activity at 20 °C. The highest activity was observed with Au/ZnO, which showed the smallest, homogeneously dispersed, Au nanoparticles (2–5 nm), in comparison with the other samples. Other researchers believe that Au/ZnO catalysts could be the best candidates for the removal of CO from hydrogen-rich fuel gases [21,22,24,25]. During 500 h of continuous experimental investigation for CO selective removal at 353 K, it was shown that the Au/ZnO catalyst had good stability [21,23]. Although its performance slightly decreased when the time-on-stream exceeded 350 h, addition of a small amount of Pt to Au/ZnO improved its stability [23]. Other authors showed that Au/ZnO catalysts retained full conversion and selectivity for long-term PROX reactions and repetitive cycles [25].

In this work, three different ZnO samples were used as supports for Au: two commercial ZnO supports (from Evonik and Strem), along with a ZnO sample consisting of nanosized tetrapods prepared by chemical vapour deposition (CVD). Gold was loaded by three different methods: photodeposition (PD), double impregnation (DIM) and ultrasonication (US). Concerning the first, only few reports exist on photodeposition of Au, and all of them refer to TiO_2 supports [36–42]. However, PD proved to be an efficient and simple method for metal deposition over semiconductor materials, causing simultaneous reduction in the metal ions by conduction band electrons of the semiconductor [43,44]. The rate of photodeposition can be enhanced by addition of "sacrificial electron donors" that can supply an almost unlimited number of electrons [44,45]. The reason why this technique has been scarcely used is related to the production of less active catalysts than other traditional techniques, such as deposition–precipitation [36–38].

* Corresponding author. Fax: +351 225081449.
** Corresponding author. Fax: +3335 34323596.
E-mail addresses: sonia.carabineiro@fe.up.pt (S.A.C. Carabineiro), Philippe.Serp@ensiacet.fr (P. Serp).

0021-9517/$ - see front matter © 2010 Elsevier Inc. All rights reserved.
doi:10.1016/j.jcat.2010.05.011

The origin of this low activity can be ascribed to both the size and shape of the gold particles produced by the photodeposition method, which are large and spherical, whereas those prepared by other methods are typically smaller than 5 nm in diameter and hemispherical in shape [46]. Consequently, for the same Au loading, one obtains lower dispersions and smaller contact perimeter between Au and the support, both of which are thought to be critical parameters in determining the overall activity [37]. However, some authors reported on the production of 1.5–5 nm particles of Au by PD on TiO_2 [37,40]. These promising results on TiO_2, and the fact that PD of Au on ZnO was never tested before, to the best of our knowledge, prompted us to prepare Au/ZnO catalysts by this method. Other less usual methods were also used for the preparation of our samples, namely, US (sonication for an established period of time). As for the DIM method, as far as we know, it has only been used for the preparation of Au/TiO_2 samples [47] and Au/ceria catalysts [48].

All the Au/ZnO samples prepared were tested in the oxidation of CO, which is an established model reaction to evaluate Au catalysts, not just due to its simplicity, but because it has potential applications, namely in CO removal from H_2 streams for fuel cells and gas sensing [1,2].

2. Experimental

2.1. Catalyst preparation

2.1.1. ZnO supports

The ZnO prepared by chemical vapour deposition (ZnO_{CVD}) was synthesised according to a previously described procedure [49,50]. Two commercial ZnO samples were used for comparison purposes: one from Strem Chemicals (ZnO_{SC}; 85–95% ZnO, 3–7% Al_2O_3, 0.5–3% CaO) and another from Evonik (ZnO_{EV}; AdNano VP 20, aggregated nanoparticles of hydrophilic ZnO). These supports were treated at 400 °C, in N_2, for 2 h, as it was found that their activity for CO oxidation (with or without Au) improved when compared with the "as received" samples.

In order to study the influence of the alumina present in ZnO_{SC}, a physical mixture of ZnO_{EV} with 10% γ-alumina (Sigma Aldrich) was also prepared and loaded with Au by the methods described below.

2.1.2. Au/ZnO materials

Au was loaded on the supports using $HAuCl_4{\cdot}3H_2O$ as the gold precursor (Alfa Aesar) in order to achieve approximately 1% wt. content of Au. The different methods used are described below.

2.1.3. Photodeposition (PD)

PD was carried out in the following way: the Au precursor was dissolved in water and methanol (300 mL, 15:1 ratio), mixed with the ZnO support, sonicated for 30 min, in order to improve dispersion, and photodeposited using a UV lamp (Heraeus TNN 15/32), with an emission line at 253.7 nm (ca. 3 W of radiant flux). A series of tests were carried out for the ZnO_{EV} using different pH-adjusted values (from 1 to 12), before photodeposition. Also, different photodeposition times (1 and 2 h) were used. Catalytic activity measurements for CO oxidation of these samples (described below) showed that the best results for PD of Au were obtained without pH adjustment (pH ∼ 5.5) and with a photodeposition time of 2 h. Since samples prepared with other pH values (from 1 to 10) and/or with 1 h of photodeposition showed a decrease in the activity, the other Au/ZnO samples prepared by PD were carried out under these conditions (no pH adjustment and 2 h photodeposition time).

2.1.4. Ultrasonication (US)

US was carried out in a similar manner, that is, dissolving the Au precursor in the same amount of water and methanol, just like in PD, however, the sample was sonicated for 8 h and then washed and dried.

2.1.5. Double impregnation (DIM)

The DIM method [47] is similar to traditional impregnation (the support is impregnated with a solution of $HAuCl_4$ using sonication), but using a second impregnation step with an aqueous solution of Na_2CO_3 (1 M), under constant ultrasonic stirring.

2.1.6. Washing and drying

All samples were washed repeatedly with distilled hot water, dried in the oven at ∼100 °C, overnight, and used without any further treatment.

2.2. Catalyst characterisation

2.2.1. ZnO supports

ZnO samples were analysed by N_2 adsorption at −196 °C, in a Quantachrome NOVA 4200e multi-station apparatus. Surface analysis for morphological characterisation was carried out by scanning electron microscopy (SEM), using a JEOL JSM-6301F (15 keV) electron microscope. The sample powders were mounted on a double-sided adhesive tape and observed at different magnifications under two different detection modes, secondary and back-scattered electrons. X-ray diffraction (XRD) analysis was carried out in a PAN'alytical X'Pert MPD equipped with a X'Celerator detector and secondary monochromator (Cu Kα $\lambda = 0.154$ nm, 50 kV, 40 mA; data recorded at a 0.017° step size, 100 s/step). Rietveld refinement with PowderCell software was used to identify the crystallographic phases present and to calculate the crystallite size from the XRD diffraction patterns. This method employs a modified version of the Debye–Scherrer equation to simultaneously determine the crystallite size and non-uniform strain (the model can be found in Ref. [51]).

2.2.2. Au/ZnO materials

A JEOL 2010F analytical electron microscope, equipped with a field-emission gun, was used for high-resolution transmission electron microscopy (HRTEM) investigations for the Au/ZnO_{EV} samples. The microscope was operated at 200 kV, and an energy-dispersive X-ray spectrometer (EDXS) LINK ISIS-300 from Oxford Instruments with an UTW Si–Li detector employed for the chemical analysis. The samples for TEM were prepared from a diluted suspension of nanoparticles in ethanol. A drop of suspension was placed on lacey carbon-coated Ni grid and allowed to dry in air. Z-contrast images were collected using a high-angle annular dark-field detector (HAADF), in scanning transmission mode (STEM). Au/ZnO_{SC} and Au/ZnO_{CVD} samples were analysed on a JEOL 1011 transmission electron microscope. The samples were dispersed in ethanol using an ultrasonic bath (20 °C) for 30 s. A drop of the dispersion was placed on a holey carbon film deposited on a copper grid and left to dry at ambient temperature. Particle size histograms were drawn from measurements made on 100–1000 particles, depending on the sample. Average particle sizes were calculated for all samples. The concentration of gold deposited on ZnO supports was measured by Inductively Coupled Plasma Optical Emission Spectroscopy (ICP-OES) using a Horiba Jobin Yvon Ultima 2 apparatus. The Au/ZnO powders were dissolved in aqua regia followed by the evaporation of acid and redispersion in 5 M HCl.

The metal dispersion was calculated by $D_M = (6n_s\,M)/(\rho N d_p)$, where n_s is the number of atoms at the surface per unit area ($1.15 \times 10^{19}\ m^{-2}$ for Au), M is the molar mass of gold (196.97 g

mol^{-1}), ρ is the density of gold (19.5 g cm^{-3}), N is Avogadro's number (6.023×10^{23} mol^{-1}) and d_p is the average particle size (determined by HRTEM, admitting that particles are spherical).

2.2.3. Catalytic tests

Catalytic activity measurements for CO oxidation were performed using a flow reactor. The catalyst sample (0.2 g) was placed on a quartz wool plug in a 45 cm-long silica tube with 2.7 cm i.d., inserted into a vertical furnace equipped with a temperature controller. Feed gas (5% CO, 10% O_2 in He) was passed through the catalytic bed at a total flow rate of 50 cm^3 min^{-1} (in contrast with most literature studies that use 1% vol. CO or less [1,2]). The composition of the outgoing gas stream was monitored using a gas chromatograph equipped with a capillary column (Carboxen 1010 Plot, Supelco) and a thermal conductivity detector.

3. Results and discussion

3.1. Characterisation of the supports

Table 1 shows the characterisation results for the ZnO samples. In agreement with other reports [3,6,24,49,50], the materials used in this study also revealed low surface areas. The highest surface area of 30 m^2 g^{-1} was measured for ZnO_{SC}, whereas ZnO_{CVD} showed the lowest value (17 m^2 g^{-1}). An intermediate result was obtained for ZnO_{EV} (26 m^2 g^{-1}). The crystallite size as measured using the Scherrer equation is found to be similar for all the samples. However, for the ZnO_{CVD} sample, the values obtained for crystallite sizes are not truly representative due to the anisotropy in the particle morphology which consists of tetrapods, as will be seen ahead.

The X-ray powder diffractograms of the ZnO supports are shown in Fig. 1. The results show the presence of a hexagonal structure (JCPDS 70-8072) for all the ZnO samples. Additionally, in agreement with the Strem Chemicals manufacturer information, the presence of alumina (α-Al_2O_3 phase, JCPDS 88-0826) was also detected in ZnO_{SC}. No crystalline impurities were observed with the other ZnO samples. The crystallite sizes of the ZnO samples derived from the XRD analysis are displayed in Table 1.

The structural differences between ZnO_{EV}, ZnO_{SC} and ZnO_{CVD} are evidenced in the SEM images depicted in Fig. 2. The commercial ZnO_{EV} (Fig. 2a) consists mainly of small (50–100 nm) cylindrical and spherical particles, while ZnO_{SC} (Fig. 2b) has a mixture of larger (100–500 nm) particles (shown by EDS to be ZnO) with smaller (10–20 nm diameter) "needle"-like particles (shown by EDS to be Al_2O_3). The ZnO_{CVD} sample (Fig. 2c) is composed of tetrapod-like structures, where needles grow from a faceted seed particle [49,50]. The nanorods have diameters varying from 8 to 50 nm and growing over 1 μm in length, giving them an aspect ratio of around 20–100.

3.2. Characterisation of Au/ZnO nanocatalysts

Fig. 3 shows representative TEM micrographs of Au/ZnO samples prepared by US method (images of Au/ZnO catalysts prepared by DIM and PD can be found in Supplementary material). It can be seen that small spherical particles are found on all the three supports after Au deposition. Particle size distributions evaluated from size measurements are summarised in Table 2 (the corresponding histograms can be found in Supplementary material). US and DIM methods produced smaller particle sizes (from 5 to 12 nm) than PD (8–17 nm). For all samples analysed by SAED, the diffracted spots correspond to ZnO phase (see an example in Supplementary material). Gold was not detected by this technique, possibly because it was below the detection limit. It was also not detected by XRD, most likely due to the low loading and the small particle size. However, EDXS results (Fig. 3a, inset) confirmed the presence of gold, and 0.9% wt. was obtained as a semi-quantitative analysis for the amount of Au present.

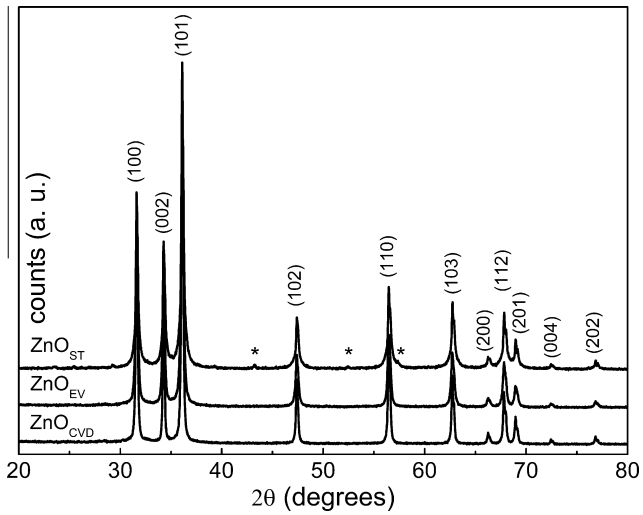

Fig. 1. X-ray diffraction spectra of ZnO_{ST}, ZnO_{EV} and ZnO_{CVD} with ZnO crystal planes identified. Alumina peaks of ZnO_{SC} are marked with *.

The gold loadings, determined by ICP-OES, are shown in Table 2; it can be seen that the values of deposited gold are near to 1% for US and PD methods, whereas deposition by DIM was less efficient (possibly due to some leaching). The values for metal dispersion (D_M) are also shown in Table 2. It can be seen that the DIM method provides the larger dispersions (as expected, since it is related with the gold loading).

For the ZnO_{SC} samples, relatively large (>10 nm) average particle sizes are obtained regardless of the preparation method. Finally, the smallest particle sizes were observed for the ZnO_{CVD} sample, irrespective of the preparation method. It is interesting to note that very small gold nanoparticles could be deposited on a low surface area support, using the DIM method. This indicates that the better control of particle sizes in the case of ZnO_{CVD} could be due to the presence of single crystals of ZnO with a high aspect ratio. This result also shows that the specific surface area is not the only determining factor for efficient particle size control in catalyst preparation.

3.3. Catalytic tests

Fig. 4 shows the CO oxidation results obtained for the pure ZnO samples and those with Au loaded by the methods described previously. The ZnO_{CVD} shows the best results among the samples without Au, achieving full CO conversion at 450 °C (Fig. 4c), in comparison with the other two supports that only attain it at ~600 °C (Fig. 4a and b). In addition, we see a significantly different behaviour for the ZnO_{CVD} sample, presumably due to important differences in the surface structure. As expected, loading the samples with Au causes CO conversion to occur at much lower

Table 1
BET surface areas and crystallite sizes of ZnO samples.

ZnO sample	BET area (m^2 g^{-1})	Crystallite size[a] (nm)
ZnO_{EV}	26	53
ZnO_{SC}	30	72
ZnO_{CVD}	17	58

[a] Average size determined by XRD.

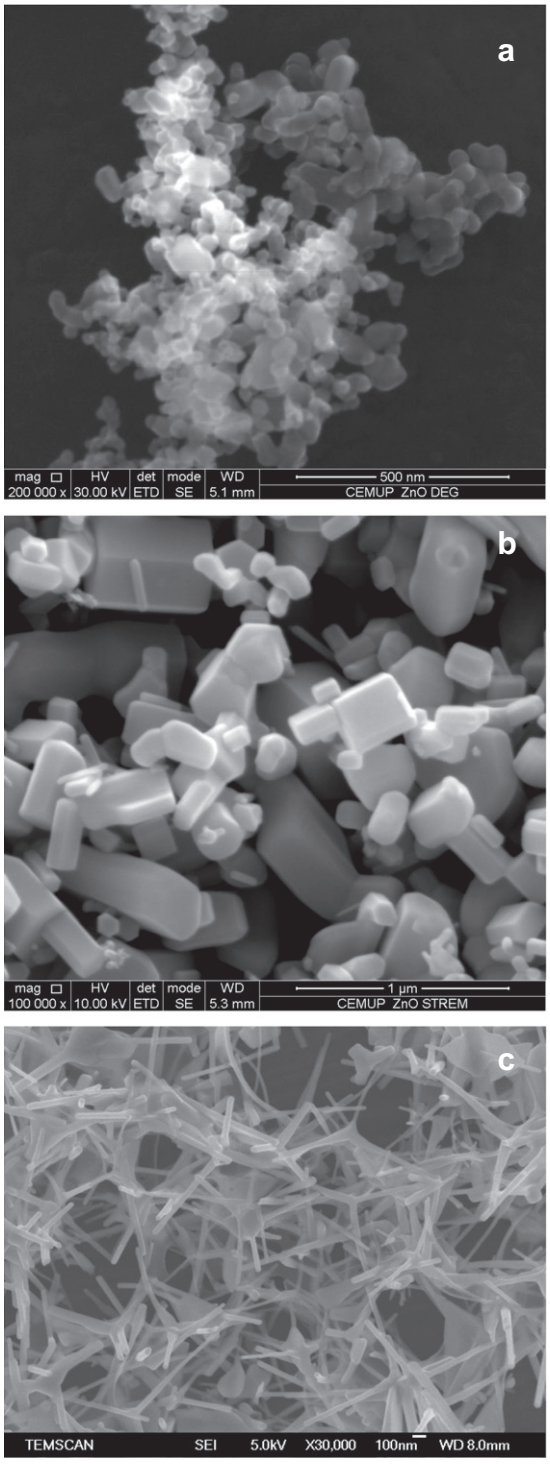

Fig. 2. SEM micrographs of (a) ZnO_{SC}, (b) ZnO_{EV} and (c) ZnO_{CVD}.

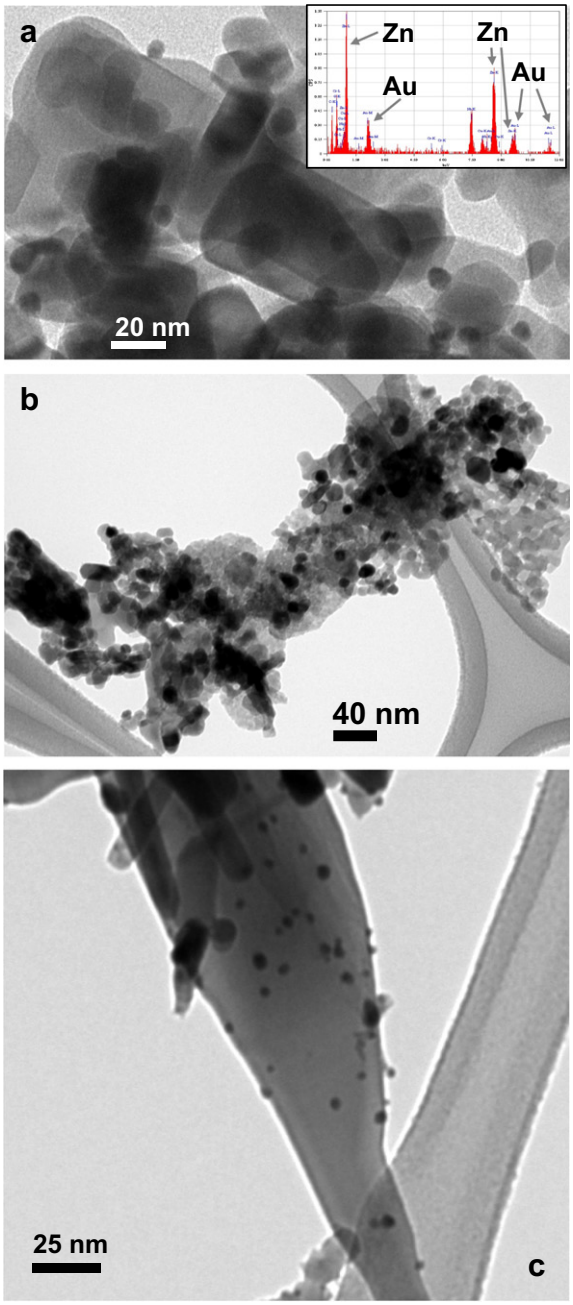

Fig. 3. TEM images of Au nanoparticles deposited on (a) ZnO_{EV}, (b) ZnO_{ST} and (c) ZnO_{CVD} by the ultrasonication (US) method. A representative EDXS spectrum of Au/ZnO system is shown in inset of (a).

temperatures. For ZnO_{EV} (Fig. 4a) and ZnO_{CVD} (Fig. 4c), the method that yields the most active samples is US (>95% conversion achieved at ~250 °C and ~150 °C, respectively), followed by DIM (near total conversion values at ~250 °C). However, for ZnO_{SC} (Fig. 4b), DIM (full conversion at ~250 °C) provides better results than US (full conversion only at ~350 °C). This can be due to the small percentage of Al_2O_3 present in this support, since it was found that the DIM method leads to better results than US both for alumina and γ-alumina loaded with Au (not shown). A physical mixture of ZnO_{EV} with 10% γ-alumina showed the same tendency.

As described in the experimental part, a series of tests were carried out for the ZnO_{EV} using different pH-adjusted values. The results obtained showed that catalysts prepared with 2 h photodeposition time and no pH adjustments (pH ~ 5.5) have higher activity. This is in agreement with what was reported by Hutchings and coworkers [18]. These authors showed that Au/ZnO catalysts can be very sensitive to pH, with materials prepared at higher pH providing lower activity [18]. In spite of the optimisation of the PD preparation carried out in this work, Fig. 4 shows that the resulting materials are not as active as those prepared by US or DIM, for any of the ZnO samples studied (since >95% conversion is only achieved at 350 °C for ZnO_{EV} and ZnO_{CVD} and 450 °C for ZnO_{SC}). Nevertheless, their catalytic behaviour was better than the ZnO support, since the activity increased up to 10

Table 2
Particle size, gold loading and metal dispersion of Au/ZnO samples prepared by different methods.

Au/ZnO sample	Au size average (nm)	Au size range[a] (nm)	Gold loading (%)	Metal dispersion (%)
Au/ZnO_{EV} US	9.5 ± 0.6	5–13	0.94	12.2
Au/ZnO_{EV} DIM	5.0 ± 0.9	2–18	0.58	23.1
Au/ZnO_{EV} PD	9.5 ± 0.6	4–20	1.26	12.2
Au/ZnO_{SC} US	11.6 ± 0.5	3–19	1.06	9.98
Au/ZnO_{SC} DIM	12.5 ± 0.1	6–20	0.74	9.26
Au/ZnO_{SC} PD	12.2 ± 0.7	4–20	1.01	9.49
Au/ZnO_{CVD} US	5.2 ± 0.9	2–11	1.01	22.3
Au/ZnO_{CVD} DIM	2.9 ± 0.9	2–14	0.72	39.9
Au/ZnO_{CVD} PD	8.3 ± 0.8	3–20	1.07	13.9

[a] See Supplementary material for the histograms.

times upon loading with Au by PD, depending on the temperature and the sample (Fig. 4).

The most active sample was found to be ZnO_{CVD} with Au loaded by US, achieving >95% conversion at ~150 °C (Fig. 4c). In addition, at room temperature, this sample is already able to convert 64% CO, which is a very high value, when compared with other samples in this study. Moreover, stability tests were carried out for this catalyst, and its activity was maintained at least for 100 h at 25 °C, and at least for 48 h at 150 °C. Comparing the specific activities at room temperature (Table 3), it can be seen that the values obtained, ranging from 0.06 to 2 $mol_{CO}\ g_{Au}^{-1}\ h^{-1}$, are higher than the value obtained for the Au/Fe_2O_3 World Gold Council reference catalyst in the same conditions (0.1 $mol_{CO}\ g_{Au}^{-1}\ h^{-1}$), with the exception of the 0.06 $mol_{CO}\ g_{Au}^{-1}\ h^{-1}$ obtained for Au/ZnO_{SC} prepared by US PD, and comparable to the value reported in literature for a $Au/ZnO/SiO_2–Na_2CO_3$ catalyst (0.464 $mol_{CO}\ g_{Au}^{-1}\ h^{-1}$) [19]. In fact, the Au/ZnO_{CVD} values are particularly high (from 0.17 to 2 $mol_{CO}\ g_{Au}^{-1}\ h^{-1}$) considering that we have a pure ZnO support, and the literature catalyst is deposited on a complex modified ZnO support. Other authors report the activities per gram of catalyst (instead of g_{Au}^{-1}). Hutchings et al. reported a rate of 6×10^{-3} $mol_{CO}\ g_{cat}^{-1}\ h^{-1}$ for a 2% Au/ZnO catalyst [15]. Our values ranging from 1×10^{-3} to 3×10^{-3} $mol_{CO}\ g_{cat}^{-1}\ h^{-1}$ (for 1% Au on ZnO_{EV} samples and 1% Au on ZnO_{CVD} prepared by DIM and PD) are within the same order of magnitude, however, the value obtained for the 1% Au/ZnO_{CVD} US catalyst, 2×10^{-2} $mol_{CO}\ g_{cat}^{-1}\ h^{-1}$, is much higher than that reported by Hutchings et al. for a 2% Au/ZnO material [15]. Activity values at other temperatures (50 °C and 100 °C), for the different Au/ZnO samples and the Au/Fe_2O_3 World Gold Council reference catalyst, are also included in Table 3, alongside with T_{50} values (temperature at which conversion is 50%) for all catalysts.

ZnO_{CVD} with Au loaded by DIM was the second best catalyst, showing 23% conversion at room temperature (Fig. 4c), while other samples did not exceed 10% (Fig. 4a and b). Surprisingly, up to 250 °C, ZnO_{EV} with Au loaded by PD (Fig. 4a) has a better performance than ZnO_{CVD} (Fig. 4c), but at 300 °C, they have similar behaviour and both achieve full conversion at 350 °C. These results are consistent with the measured Au nanoparticle sizes (Table 2).

Activation energies were also calculated and are displayed in Table 3. It can be seen that the ZnO_{CVD} shows the lowest values, specially the US and DIM samples, the most active samples in this study, that have 5 and 7 kJ mol^{-1}. Values below 10 kJ mol^{-1} were found in literature for nanoporous gold prepared by leaching silver out of the corresponding alloy [52] or by leaching from $AuCu_3$ [53], for Au sponge [54], Au/titania [55–57] and $Au/Fe(OH)_3$ [57]. Goodman and co-workers showed that the apparent activation energy for the CO oxidation reaction in the temperature range from 77 to 177 °C can vary from 7 to 21 kJ mol^{-1} as the Au particle size increases from 2.5 to 6 nm for Au/titania [58,59]. Therefore, samples

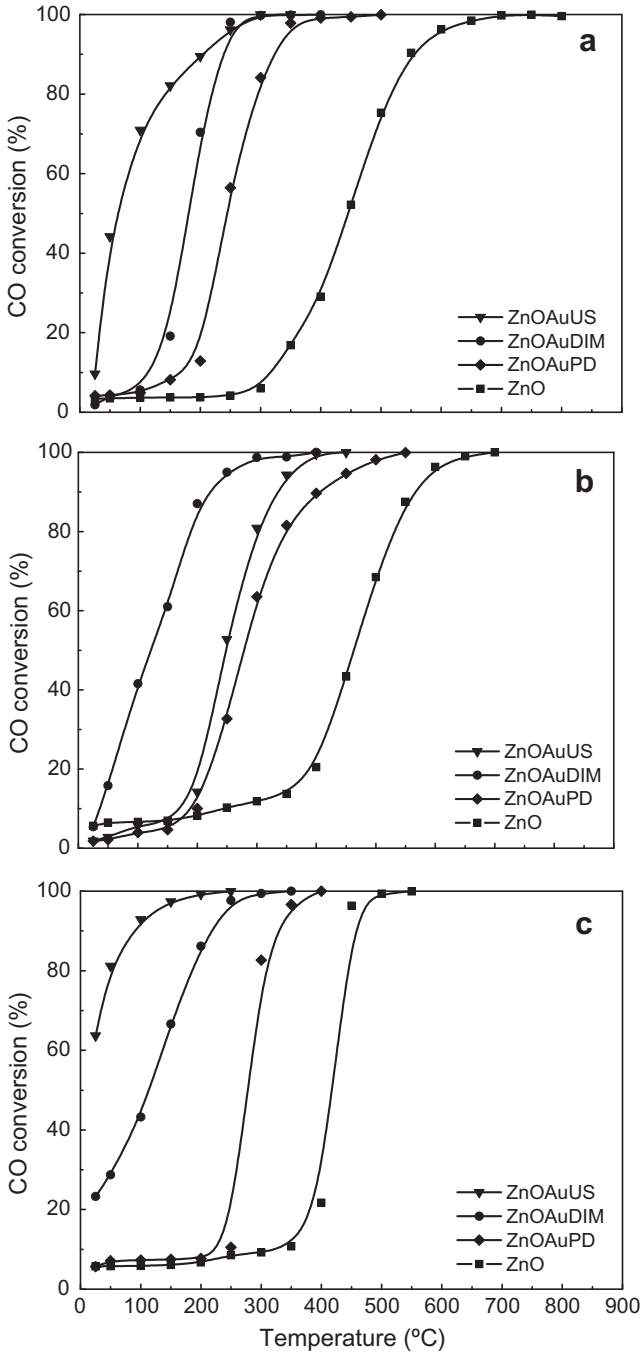

Fig. 4. CO conversion (%) versus temperature for the (a) ZnO_{EV}, (b) ZnO_{SC} and (c) ZnO_{CVD} supports alone and with Au loaded by different methods.

with smaller particle size are expected to have lower activation energy, which matches well with our results. Other samples in our work showed values between 12 and 23 kJ mol^{-1}. In literature, values around 10 kJ mol^{-1} were also found for Au/alumina [60], Au/ceria [61] and fine gold (unsupported) powder [62], and activation energies ranging from 10 to 30 kJ mol^{-1}were also reported for Au/titania [63,64], which match well with our results.

Some conclusions can be drawn from the catalytic tests. First, it is well known that Au particles of sizes above 5 nm show low activity in catalysis, and our results confirm this, irrespective of the support and the method employed for gold deposition. This is particularly well exemplified in the case of the ZnO_{SC} sample, on which large gold particles were obtained by all methods. Since this

Table 3
Activities, T_{50} and activation energies calculated for the Au/ZnO samples prepared by different methods, at different temperatures, and the Au/Fe_2O_3 World Gold Council (WGC) reference catalyst.

Au/ZnO sample	Activities ($mol_{CO}\ g_{Au}^{-1}\ h^{-1}$) at different temperatures			Activation energies ($kJ\ mol^{-1}$)	T_{50} values (°C)
	25 °C	50 °C	100 °C		
Au/ZnO_{EV} US	0.32	1.47	2.36	23	58
Au/ZnO_{EV} DIM	0.17	0.22	0.30	21	170
Au/ZnO_{EV} PD	0.12	0.13	0.14	16	242
Au/ZnO_{SC} US	0.06	0.08	0.17	13	246
Au/ZnO_{SC} DIM	0.23	0.67	1.75	18	121
Au/ZnO_{SC} PD	0.06	0.07	0.12	22	278
Au/ZnO_{CVD} US	2.00	2.51	2.87	5	<25
Au/ZnO_{CVD} DIM	1.01	1.25	1.88	7	115
Au/ZnO_{CVD} PD	0.17	0.19	0.22	17	290
Au/Fe_2O_3 WGC	0.10	0.18	0.33	20	193

is a two-phase system (Al_2O_3 + ZnO), it is difficult to control the particle size a priori. Second, the DIM preparation method yielded disappointing results in catalysis, despite a better control of particle size. This may be due to the building up of monodentate carbonate species on the catalyst surface that poison the catalyst, as already proposed for Au/TiO_2 catalyst in the CO oxidation reaction [65]. These species may be desorbed at higher temperatures, explaining the results obtained at 300 °C.

Finally, in order to understand the high activity of the Au/ZnO_{CVD} system prepared by the US method, we investigated the crystallography of this system by HRTEM. In this sample, we observed that Au particles were epitaxially grown on the ZnO support in a number of cases. An example is shown in Fig. 5a, where a HRTEM image of a partly overlapping Au particle attached to the ZnO support is shown. Inset is the Fast Fourier Transform analysis (FFT) of the HRTEM micrograph which is enlarged and indexed in Fig. 5b. We found that the ZnO-supporting particle was close to the [−2 1 1 0] zone axis and the Au particle could be indexed as [1 1 0] zone axis. It was found that the d values for [0 0 2] of gold (as indexed on FFT image with open circles and labelled with white numerals) deviate (are larger) from the original value by around 10%. Values for (1 1 1) planes were found to be within less than 5%. Detailed analysis also showed that there was some angle deviation between the planes of Au and ZnO (2–5°). This could be explained by the deviation from ideal epitaxy or a slight bending of the investigated area of the sample. From this and similar cases, the following crystallographic relations could be concluded: Parallel directions: [1 1 0] Au//[−2 1 1 0] ZnO and parallel planes: (−1 1 −1) Au//(0 0 0 1) ZnO. Apart from that, relations (within few degrees) were found for (1 −1 −1) Au//(0 1 −1 −1) ZnO and (0 0 1) Au//(0 −1 1 −1) ZnO. These results are in good agreement with previously reported epitaxial growth of Au on ZnO or ZnO on Au substrates [66–68]. We can propose that epitaxial growth of Au particles on ZnO influenced the particle size and that the strong metal–support interaction may result in the improvement of the catalytic properties of the sample. No epitaxy was found for any of the other samples.

As for the CO oxidation mechanism, although it has been extensively studied in several catalysts, it is still under debate [1,2,69,70]. For gold supported on an oxide, it is widely accepted that a CO molecule is chemisorbed on a gold atom, while an hydroxyl ion moves from the support to a Au(III) ion, creating an anion vacancy. They react to form a carboxylate group, and an oxygen molecule occupies the anion vacancy as O_2^-. This oxidises the carboxylate group by extracting a hydrogen atom, forming carbon dioxide, and the resulting hydroperoxide ion HO_2^- then oxidises a further carboxylate species forming another carbon dioxide and restoring two hydroxide ions to the support surface, completing the catalytic cycle. This mechanism was proposed in 2000 by Bond and Thompson [69] and has been substantiated by subsequent results of several authors [70]. Exceptions are, naturally, some "inert" supports like alumina and silica, where oxygen chemisorption will be negligible and involvement of lattice oxide ions is unlikely; therefore, the mechanism on gold particles, where there is no support participation and where the total perimeter is comparatively small, will be of the Langmuir–Hinshelwood type, involving oxygen (weakly) and carbon monoxide (more strongly) adjacently adsorbed onto gold [69].

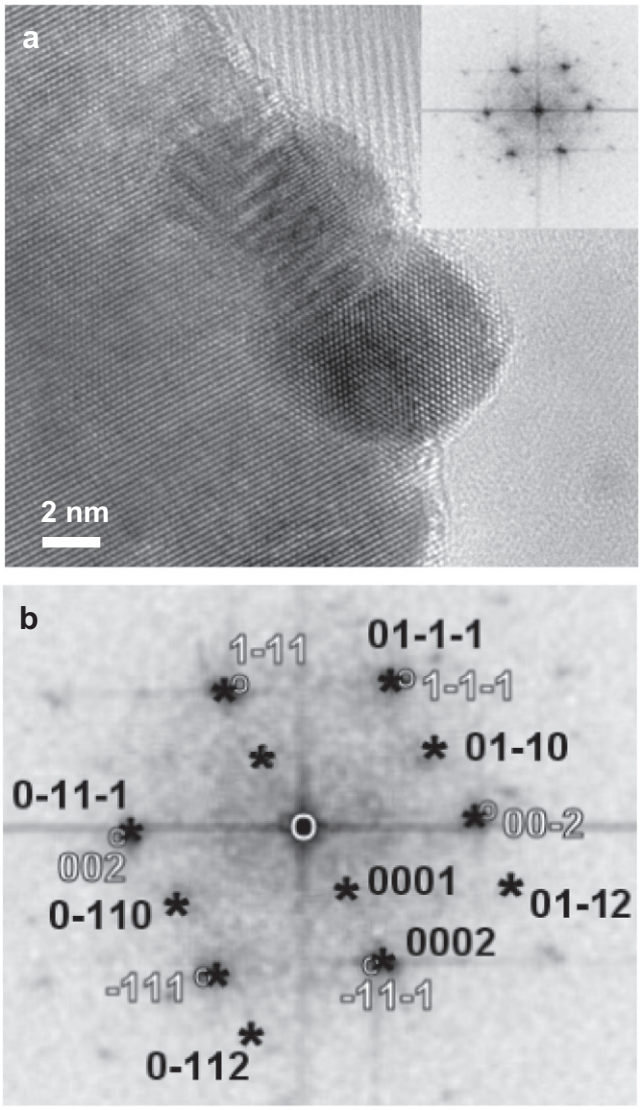

Fig. 5. (a) HRTEM micrograph of an epitaxially grown Au particle on ZnO support with FFT as inset and (b) indexed "diffraction spots" in FFT image (open circles and white numerals correspond to Au; black numerals and asterisks are used to label ZnO planes).

The Bond and Thompson mechanism suggests that it is the lattice oxygen of the support that reacts with CO and that the O_2 provided is only needed to restore the support surface. Therefore, the reaction greatly depends on the strength of interaction with the support [36]. Since other supports, like TiO_2, provide a stronger metal–support interaction effect [71] that can also explain the better catalytic behaviour of Au/TiO_2 systems described in the literature, when compared to Au/ZnO. Nevertheless, our results with the Au/ZnO_{CVD} sample prepared by US show a remarkable performance when compared with the few results available in the literature, as explained earlier.

To summarise, we have seen in this study that the ZnO_{CVD} support presents a different surface structure leading to better particle size distribution and higher activity with or without gold deposition. In the Au/ZnO_{CVD} system, HRTEM analysis provides useful information showing that an unexpected strong metal–support interaction can exist, since gold can have an epitaxial relation to the ZnO single crystal. This interaction can have a direct impact on the gold particle size distribution and the electronic properties. More studies are required for a quantitative evaluation of these interactions.

4. Conclusions

One percent weight Au was loaded on three different ZnO supports (two commercial, from Evonik and Strem, and one prepared by CVD), by three different methods: PD, DIM and US, and the materials were used for the oxidation of CO. It was found that small gold particles can be deposited on a low surface area support using the US and DIM methods and that the surface structure of the support has a profound influence on the particle size distribution. In particular, the most active sample was prepared using the ZnO_{CVD}, with Au loaded by US, that showed an activity of 2 $mol_{CO}\ g_{Au}^{-1}\ h^{-1}$ at room temperature, which is among the best values so far reported for this reaction on Au/ZnO-type catalysts. This high activity can be due to the unique metal–support interactions present in this system (Au particles were epitaxially grown on ZnO support) that were not found for the other catalysts in this work.

Acknowledgments

Fundação para a Ciência e Tecnologia (FCT), Portugal, and the Ministry of Higher Education, Science and Technology, Slovenia, for financial support through the Portugal–Slovenia Cooperation in Science and Technology (2008/2009). FCT is also acknowledged for financing for LSRE/LCM Associate Laboratory (“Programa de Financiamento Plurianual de Unidades de I&D/Laboratórios Associados”) and for SAC (CIENCIA 2007 program). RB and PS gratefully acknowledge research funding from Agence Nationale de Recherche, France (RNMP05-PRONANOX). Authors acknowledge P. Besson (LMTG – UMR 5563 CNRS, Toulouse) for the ICP-OES analysis of gold and are grateful to Evonik Spain (Mr. Juán Manuel Flores) for the free ZnO (VP AdNano 20) sample provided.

Appendix A. Supplementary material

Supplementary data associated with this article can be found, in the online version, at doi:10.1016/j.jcat.2010.05.011.

References

[1] S.A.C. Carabineiro, D.T. Thompson, Nanocatalysis, in: U. Heiz, U. Landman (Eds.), Springer-Verlag, Berlin, Heidelberg, New York, 2007, pp. 377–489. ISBN-13 978-3-540-32645-8.
[2] S.A.C. Carabineiro, D.T. Thompson, Gold: Science and Applications, in: C. Corti, R. Holliday (Eds.), CRC Press, Taylor and Francis Group, Boca Raton, London, New York, 2010, pp. 89–122. ISBN-978-1-4200-6523-7.
[3] J. Strunk, K. Kähler, X. Xia, M. Comotti, F. Schüth, T. Reinecke, M. Muhler, Appl. Catal. A: Gen. 359 (2009) 121–128.
[4] M. Manzoli, A. Chiorino, F. Boccuzzi, Appl. Catal. B: Environ. 57 (2005) 201–209.
[5] A. Ueda, T. Oshima, M. Haruta, Appl. Catal. B: Environ. 12 (1997) 81–93.
[6] H. Sakurai, S. Tsubota, M. Haruta, Appl. Catal. A: Gen. 102 (1993) 125–136.
[7] H. Sakurai, M. Haruta, Appl. Catal. A: Gen. 127 (1995) 93–105.
[8] J.E. Bailie, G.J. Hutchings, Chem. Commun. (1999) 2151–2152.
[9] J.E. Bailie, H.A. Abdullah, J.A. Anderson, C.H. Rochester, N.V. Richardson, N. Hodge, J.-G. Zhang, A. Burrows, C.J. Kiely, G.J. Hutchings, Phys. Chem. Chem. Phys. 3 (2001) 4113–4121.
[10] P. Landon, P.J. Collier, A.J. Papworth, C.J. Kiely, G.J. Hutchings, Chem. Commun. (2002) 2058–2059.
[11] C. Milone, R. Ingoglia, A. Pistone, G. Neri, S. Galvagno, Catal. Lett. 87 (2003) 201–209.
[12] N.S. Patil, B.S. Uphade, D.G. McCulloh, S.K. Bhargava, V.R. Choudhary, Catal. Commun. 5 (2004) 681–685.
[13] J.-J. Wu, C.-H. Tseng, Appl. Catal. B: Environ. 66 (2006) 51–57.
[14] F. Boccuzzi, A. Chiorino, S. Tsubota, M. Haruta, Catal. Lett. 29 (1994) 225–234.
[15] G.J. Hutchings, M.R.H. Siddiqui, A. Burrows, C.J. Kiely, R. Whyman, J. Chem. Soc. Faraday Trans. 93 (1997) 187–188.
[16] G.Y. Wang, W.X. Zhang, H.L. Lian, D.Z. Jiang, T.H. Wu, Appl. Catal. A: Gen. 239 (2003) 1–10.
[17] M. Comotti, W.-C. Li, B. Spliethoff, F. Schuth, J. Am. Chem. Soc. 128 (2005) 917–924.
[18] S. Al-Sayari, A. Carley, S. Taylor, G. Hutchings, Top. Catal. 44 (2007) 123–128.
[19] K. Qian, W. Huang, J. Fang, S. Lv, B. He, Z. Jiang, S. Wei, J. Catal. 255 (2008) 269–278.
[20] T. Tabakova, V. Idakiev, D. Andreeva, I. Mitov, Appl. Catal. A: Gen. 202 (2000) 91–97.
[21] J. Zhang, Y. Wang, B. Chen, C. Li, D. Wu, X. Wang, Energy Convers. Manage. 44 (2003) 1805–1815.
[22] M. Manzoli, A. Chiorino, F. Boccuzzi, Appl. Catal. B: Environ. 52 (2004) 259–266.
[23] Y.H. Wang, J.L. Zhu, J.C. Zhang, L.F. Song, J.Y. Hu, S.L. Ong, W.J. Ng, J. Power Sources 155 (2006) 440–446.
[24] K.R. Souza, A.F.F. de Lima, F.F. de Sousa, L.G. Appel, Appl. Catal. A: Gen. 340 (2008) 133–139.
[25] H. Imai, M. Daté, S. Tsubota, Catal. Lett. 124 (2008) 68–73.
[26] P. Naknam, A. Luengnaruemitchai, S. Wongkasemjit, Energy Fuels 23 (2009) 5084–5091.
[27] P. Naknam, A. Luengnaruemitchai, S. Wongkasemjit, Int. J. Hydrogen Energy 34 (2009) 9838–9846.
[28] F. Boccuzzi, A. Chiorino, S. Tsubota, M. Haruta, Sens. Act. B: Chem. 25 (1995) 540–543.
[29] S.-J. Chang, T.-J. Hsueh, I.-C. Chen, B.-R. Huang, Nanotechnology 19 (2008) 175502.
[30] R.K. Joshi, Q. Hu, F. Am, N. Joshi, A. Kumar, J. Phys. Chem. C 113 (2009) 16199–16202.
[31] C. Wongchoosuk, S. Choopun, A. Tuantranont, T. Kerdcharoen, Mater. Res. Innov. 13 (2009) 185–188.
[32] G. Socol, E. Axente, C. Ristoscu, F. Sima, A. Popescu, N. Stefan, I.N. Mihailescu, L. Escoubas, J. Ferreira, S. Bakalova, A. Szekeres, J. Appl. Phys. 102 (2007) 083103.
[33] Ch. Pandis, N. Brilis, E. Bourithis, D. Tsamakis, H. Ali, S. Krishnamoorthy, A.A. Iliadis, M. Kompitsas, IEEE Sens. J. 7 (2007) 448–454.
[34] R. Mishra, K. Rajanna, Sens. Mater. 17 (2005) 433–440.
[35] H.P. Yang, S.G. Chen, C.H. Li, D.C. Chen, Z.C. Ge, Prog. Chem. 21 (2009) 210–216.
[36] G.R. Bamwenda, S. Tsubota, T. Nakamura, M. Haruta, Catal. Lett. 44 (1997) 83–87.
[37] C.-y. Wang, C.-y. Liu, X. Zheng, J. Chen, T. Shen, Colloids Surf. A: Physicochem. Eng. Aspects 131 (1998) 271–280.
[38] S.C. Chan, M.A. Barteau, Langmuir 21 (2005) 5588–5595.
[39] P. He, M. Zhang, D. Yang, J. Yang, Surf. Rev. Lett. 13 (2006) 51–55.
[40] L.-H. Chang, Y.-L. Yeh, Y.-W. Chen, Int. J. Hydrogen Energy 33 (2008) 1965–1974.
[41] C. Yogi, K. Kojima, T. Takai, N. Wada, J. Mater. Sci. 44 (2009) 821–827.
[42] P. Sangeetha, L.H. Chang, Y.W. Chen, Ind. Eng. Chem. Res. 48 (2009) 5666–5670.
[43] Z. Zhang, C.-C. Wang, R. Zakaria, J.Y. Ying, J. Phys. Chem. B 102 (1998) 10871–10878.
[44] B.F. Machado, Ph.D. Thesis in Chemical Engineering, University of Porto, 2008.
[45] M.I. Litter, Appl. Catal. B: Environ. 23 (1999) 89–114.
[46] M. Haruta. Gold as a novel catalyst in the 21st century: preparation, working mechanism and applications, in: Gold 2003 Conference, Vancouver, Canada, 2003.
[47] M. Bowker, A. Nuhu, J. Soares, Catal. Today 122 (2007) 245–247.
[48] S.A.C. Carabineiro, A.M.T. Silva, G. Dražić, P.B. Tavares, J.L. Figueiredo, Catal. Today, in press, doi:10.1016/j.cattod.2010.01.036.
[49] R. Bacsa, Y. Kihn, M. Verelst, J. Dexpert, W. Bacsa, P. Serp, Surf. Coatings Technol. 201 (2007) 9200–9204.
[50] R.R. Bacsa, J. Dexpert-Ghys, M. Verelst, A. Falqui, B. Machado, W.S. Bacsa, P. Chen, S.M. Zakeeruddin, M. Graetzel, P. Serp, Adv. Funct. Mater. 19 (2009) 875–886.
[51] K.A. Thomas, P.S.I.P.N. de Silva, L.F. Cohen, A. Hossain, M. Rajeswari, T. Venkatesan, R. Hiskes, J.L. MacManus-Driscoll, J. Appl. Phys. 84 (1998) 3939–3948.
[52] A. Wittstock, B. Neumann, A. Schaefer, K. Dumbuya, C. Kübel, M.M. Biener, V. Zielasek, H.-P. Steinrück, J.M. Gottfried, J. Biener, A. Hamza, M. Baümer, J. Phys. Chem. C 113 (2009) 5593–5600.
[53] S. Kameoka, A.P. Tsai, Catal. Lett. 121 (2008) 337–341.
[54] N.W. Cant, P.W. Fredrickson, J. Catal. 37 (1975) 531–539.
[55] Y. Iizuka, T. Tode, T. Takao, K.i. Yatsu, T. Takeuchi, S. Tsubota, M. Haruta, J. Catal. 187 (1999) 50–58.
[56] S.H. Overbury, V. Schwartz, D.R. Mullins, W. Yana, S. Dai, J. Catal. 241 (2006) 56–65.
[57] M. Olea, M. Tada, Y. Iwasawa, J. Catal. 248 (2007) 60–67.
[58] M. Valden, X. Lai, D.W. Goodman, Science 281 (1998) 1647–1650.
[59] M. Valden, S. Pak, X. Lai, D.W. Goodman, Catal. Lett. 56 (1998) 7–10.
[60] J.T. Calla, R.J. Davis, J. Phys. Chem. B 109 (2005) 2307–2314.

[61] U.R. Pillai, S. Deevi, Appl. Catal. A: Gen. 299 (2006) 266–273.
[62] Y. Iizuka, H. Fujiki, N. Yamauchi, T. Chijiiwa, S. Arai, S. Tsubota, M. Haruta, Catal. Today 36 (1997) 115–123.
[63] S. Tsubota, T. Nakamura, K. Tanaka, M. Haruta, Catal. Lett. 56 (1998) 131–135.
[64] M. Haruta, Cattech 6 (2002) 102–115.
[65] K.Y. Ho, K.L. Yeung, Gold Bull. 40 (2007) 15–30.
[66] E.F. Wassermann, K.A. Polacek, Surf. Sci. 28 (1971) 77–83.
[67] R. Liu, A.A. Vertegel, E.W. Bohannan, T.A. Sorenson, J.A. Switzer, Chem. Mater. 13 (2001) 508–512.
[68] S.J. Limmer, E.A. Kulp, J.A. Switzer, Langmuir 22 (2006) 10535–10539.
[69] G.C. Bond, D.T. Thompson, Gold Bull. 33 (2000) 41–51.
[70] G.C. Bond, D.T. Thompson, Gold Bull. 42 (2009) 247–259.
[71] S.J. Tauster, S.C. Fung, R.L. Garten, J. Am. Chem. Soc. 100 (1978) 170–175.